Colloid Polym Sci 279:252–258 (2001)

ORIGINAL CONTRIBUTION

S. Fujii
T. Isojima
N. Sasaki
K. Hamano

Dynamic light scattering of an ionic SDS micellar solution under an AC electric field

Received: 9 June 2000
Accepted: 31 August 2000

S. Fujii · T. Isojima · N. Sasaki
K. Hamano
Department of Biological and
Chemical Engineering
Faculty of Technology
Gunma University, Kiryu, Japan

S. Fujii (✉)
Division of Biological Sciences
Graduate School of Science
Hokkaido University, Kita-ku
Sapporo 060–0810, Japan
e-mail: fujii@gogh.sci.hokudai.ac.jp
Tel.: +81-11-7063809
Fax: +81-11-7064992

Present address:
S. Fujii · N. Sasaki
Division of Biological Sciences
Graduate School of Science
Hokkaido University, Kita-ku
Sapporo 060–0810, Japan

In the course of the preparation of this paper, Prof. Hamano died from sudden heart failure.

Abstract The phase separation behavior of near-critical ionic sodium-dodecyl-sulfate (SDS) micellar solution under a sinusoidal electric field was investigated by phase-contrast optical microscopy and by the small-angle dynamic light scattering method. The sinusoidal electric field significantly deformed the concentration domains and shifted the phase separation temperature. The autocorrelation function under a sinusoidal electric field was measured in the vicinity of a phase separation temperature range of $0.10\ K < T_p - T < 0.97\ K$, where $T_p - T$ is the temperature distance from the phase separation temperature in quiescent state T_p. The correlation function with an oscillatory part in the longer correlation time region was observed. The occurrence of the oscillatory mode, which depended on both the applied field frequency and the ambient temperature, indicates deformation of concentration fluctuation domains by dynamical coupling between the phase separation and the applied sinusoidal electric field.

Key words Critical point · Binary mixtures · Phase separation · Light scattering · Electric field-induced phenomena · Concentration domain

Introduction

The phase separation behavior of micellar systems near the critical point belongs to the universality of a usual binary mixture system. We have studied phase separation phenomena of micellar solution systems on the basis of the general theory of critical phenomena [1]. A critical phenomenon, which is independent of constituents of a system, is governed by the universality to describe a phase separation phenomenon. Many researchers have investigated binary mixture systems, such as a polymer solution, micellar solution, gel, and liquid crystal, to which the universality is applicable. Recently, the concept of critical dynamics has been applied to phase separation under external force because of the possibility of a dynamical coupling phenomenon between critical fluctuation and external force. If external force is combined with critical fluctuation, it will be very interesting to know whether the universality can still be applied to a phase separation phenomenon under an external field [2–6]. It has been reported that an external force, such as an electric field, a shear flow, or an acoustic wave, deforms critical fluctuation [2–8, 12]. The deformation of critical fluctuation causes changes in

various phase separation behaviors. In particular, a nonionic micellar solution in a shear flow has been known to manifest different phase separation behavior to that of an ionic micellar solution in a shear flow. In the case of a nonionic micellar solution, when shear flow was applied to the mixture near critical point, the critical fluctuation was broken and shear-induced homogenization occurred [3–5, 9, 10]. On the other hand, in an ionic micellar solution, shear flow generates an increase in the inhomogeneous concentration distribution [10], and a shear-induced phase separation occurs [11]. This fact indicates that the distribution of charges in the system affects the phase separation behavior through the dynamic coupling phenomena. The electrostatic interaction seems to play an important role. Although phase separation under an electric field has been studied both experimentally and theoretically, information is still limited [6, 14, 15]. In order to obtain information on electrostatic interaction, phase separation behavior of an ionic micellar solution was investigated under an AC electric field. We have employed an ionic sodium-dodecyl-sulfate (SDS) micellar system that has ζ potential on the surface of the micelle [13].

An SDS micellar solution is a typical solution that has a pair of demixing temperatures, namely, lower and upper demixing points. As the SDS micelle has a negative surface potential, the addition of salt to the solution changes the two demixing temperatures; the difference between the upper and lower demixing temperatures becomes small as the salt concentration decreases. This change is attributed to the electrostatic screening effect of Na^+, which makes the van der Waals interaction between SDS molecules more effective. The upper phase-separation temperature increases as the salt concentration increases. On the other hand, at the lower demixing point, Na^+ weakens the hydrogen bond by shielding polar groups of the SDS micelles from H_2O. As a result, the lower demixing temperature decreases with increases in the salt concentration. The dynamical behavior of this system has been characterized in detail and has been explained by the modified dynamical droplet model under the assumption that thermally activated local fluctuation behaves as physical clusters with a fractal dimension of $d_f = 2.49$ and a polydispersity exponent of $\tau = 2.21$, together with an effective micellar size of about $7 \sim 8$ nm [16].

In this article, we present experimental results of (1) morphological observations of the concentration domain and (2) correlation function determination by the small-angle dynamic light scattering method, both under a sinusoidal electric field.

Experimental

We employed an aqueous solution of an ionic sodium-dodecyl-sulfate (SDS), butanol, and NaCl, where weight fractions of SDS and butanol in the aqueous solution were 0.0460 and 0.0813, respectively. As described in Introduction, the phase diagram of the SDS mixture has an immiscibility gap with a loop size of $\Delta T = T_U - T_L$ that depends on the NaCl concentration, where T_U and T_L are the upper and lower demixing temperatures [16], respectively. Since the SDS micelles have a surface charge (ζ-potential) that causes coulombic interaction between the micelles in the mixture, T_L decreases and T_U increases with increases in the salt concentration. The two branches of the phase boundary appear much closer at a low NaCl concentration. At NaCl concentrations of less than 0.0580 in weight fraction, the mixture is completely miscible. In this study, all experiments were performed in the vicinity of a lower consolute temperature $T_L \simeq 12.79_8$ °C and at an NaCl concentration of 0.0660. SDS, butanol, and NaCl were purchased from Wako Pure Chemical Industries, Ltd. Sample preparation was carried out in a dry box filled with dry nitrogen to prevent oxidation.

The cloud point in the quiescent state was determined by observing the appearance of a characteristic forward light scattering pattern, i.e., a spinodal ring.

Concentration domain morphology during the phase separation under a sinusoidal electric field was observed under a phase contrast optical microscope Nikon-microphoto-FXA. The microscopy image was recorded in an optical micrograph. The homemade sample cell used to apply an electric field to the sample solution has approximate dimensions of $10 \times 4 \times 1$ mm, and the gap between the electrodes is about 1.5 mm. The sample cell was set in a heat jacket made of brass mounted on the microscope stage, and the temperature of the sample solution was controlled to within ± 10 mK by circulating thermostated water through the heat jacket. The electric field for excitation was generated by a Kenwood AG-204 oscillator. In this observation, the electric field was applied to the solution at a frequency of $f = 1$ kHz and a driving voltage of $E = 3.3$ V/cm.

Dynamical measurements were performed with a homemade small-angle light scattering apparatus using an He-Ne laser ($\lambda_0 = 632.8$ nm, 10 mW). Dynamic light scattering measurements under an electric field were carried out using a similar method to that of Ware and Flygare [21, 22]. The sample cell was immersed in a temperature-regulated water bath, the temperature of which was monitored by a quartz thermometer with an accuracy of ± 2 mK. A photomultiplier tube detector (PMD) was mounted on the rail of a goniometer, which has a half circle track with a radius of 50 cm, and the sample cell was placed in the center of the half circle. The PMD moves on the rail to detect the scattered light at any scattering angle. The scattered light detected at an arbitrary angle was analyzed by the photon-counting method. Measurements of the correlation function were performed with the homodyne mode [23] using a multi-τ photon correlator "BI-9000AT" manufactured by BrookHaven Corporation. Calibration of the scattering angle of the goniometer was made using the suspension of polystyrene latex with a radius of 44.5 nm. The detector was fixed at the geometric angle of $\theta = 3.0°$ against the incident beam. Figure 1 shows the autocorrelation function obtained for the polystyrene latex suspension using the small angle light scattering apparatus. The radius estimated from the small-angle light scattering experiment was $r = 43$ nm and, according to the Einstein-Stokes relation, the corrected angle was $\theta = 3.1°$ with accuracy. In these experiments, the detecting angle θ was fixed at $\theta = 3.1°$ and wave vector $q = 6.9_1 \times 10^3$ cm^{-1}. In Fig. 1, a fast decay of about 10^{-2} s could be observed in the correlation function. As the appearance of the fast decay depended on the set-up of the optical path, we considered that the fast decay was caused by imperfections in the collimation of the small angle optical system. Estimation of the radius of a polystyrene latex bead was performed disregarding the fast mode. The estimated radius was 43 nm, which is very similar to the well-defined radius of a polystyrene latex bead, $r = 44.5$ nm, as mentioned above. This fact indicates that disregarding the fast

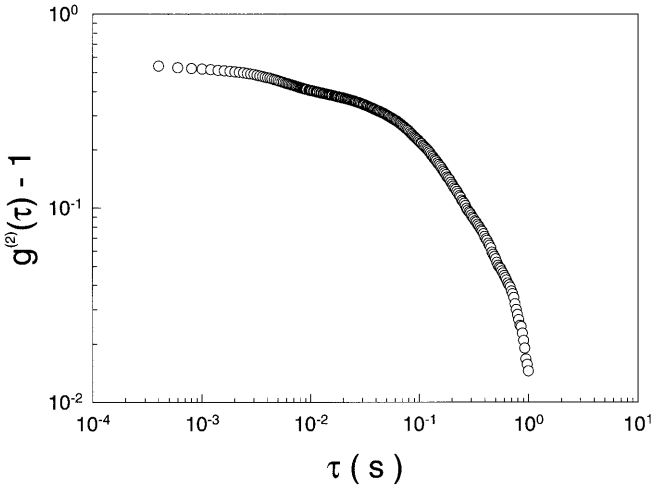

Fig. 1 The correlation function for a suspension of latex particles whose radius r is r = 44.5 nm. The angular resolution of the small-angle light scattering apparatus was quantified

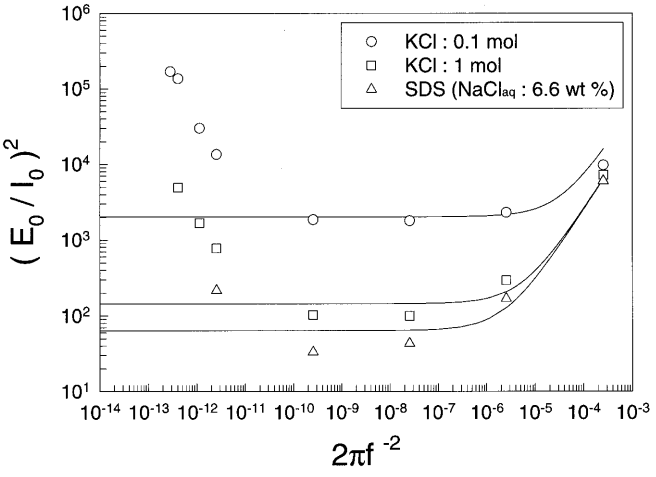

Fig. 2 Determination of the apparatus constant of the ZetaPlus Brookhaven gold electrodes in each solution. *Circles*, *squares*, *and triangles* show 0.1 mol KCl_{aq}, 1 mol KCl_{aq}, and SDS mixtures. The *solid lines* represent the theoretical curve (Eq. 1) for the circuit used in this experiment

decay mode does not have a significant effect on the correlation function, at least in the slow decay mode. Therefore, in the following, the fast decay mode is not considered. Even if the fast decay mode affected the correlation function, it would not influence the qualitative analysis for the damping oscillation in the correlation function, as shown in Fig. 6.

The sample cell used for light scattering measurement was made of Pyrex glass and had inside dimensions of $10 \times 10 \times 45$ mm. We equipped the sample cell with rectangular electrodes in order to apply an electric field to the sample solution. The electrodes were similar to those used by Uzgiris [17]. The electrodes, purchased from the ZetaPlus Brookhaven electrodes of Brookhaven Corporation, were made of gold. The electrodes had a rectangular shape of 5.0 (width) × 8.5 (length) × 0.4 (thickness) mm, and they were set parallel at a distance of 3.5 mm. Since the electrodes had no contact with the Pyrex glass cell and were entirely surrounded by the sample solution, there was no possibility of the occurrence an electroosmosis phenomenon on the surface of the glass. Hence, it was possible to measure the dynamically coupling phenomenon between electrophoretic and concentration fluctuations of the micellar solution without an electroosmosis flow of solution on the surface of the glass. In the measurement of dynamic light scattering, an electric field was applied perpendicular to an incident beam. The electric properties of the solution would be governed by the geometrical shape of the electrodes and the species of the electrodes. In order to determine an appropriate frequency range for measuring dynamic light scattering, we calibrated the electrodes using 0.1 mol/l and 1 mol/l KCl aqueous solutions and an ionic SDS micellar solution that was identical to the sample solution used in this work. Calibration was performed in the range of frequency f from 10 Hz–300 kHz at T = 25 °C. In the calibration, for simplification, we assumed that the power supply and the sample cell with electrodes were connected in series in our electric circuit.

The results of calibration are shown in Fig. 2. The solid line represents the theoretical curve for the electric circuit used in this experiment:

$$\frac{E_0}{I_0} = \frac{1}{C^2}(2\pi f)^{-2} + R^2 \qquad (1)$$

where E_0, I_0 and f are amplitude voltage, amplitude current, and frequency of the electricity, respectively. C and R are capacitance (F) and resistance (Ω) for these solutions, respectively. Experimental data were well described by the theoretical relation in the range of frequency from 100 Hz–10 kHz. By fitting the data with the theoretical relation using the method of least-squares in the frequency range determined above, we were able to obtain the capacitance C and resistance R, as the electric properties of the sample solutions. In an SDS micellar solution, the electric properties were C = 205.8 (μF) and R = 7.839 (Ω). Similarly, in 0.1 mol/l KCl_{aq} the properties were C = 179.6 (μF) and R = 44.35 (Ω), and in 1 mol/l KCl_{aq} they were C = 195.8 (μF) and R = 11.97 (Ω). The lower frequencies for the appropriate fitting of an SDS micellar solution, 0.1 mol/l of KCl_{aq} and 1 mol/l of KCl_{aq}, were f = 80 Hz, 20 Hz, and 70 Hz, respectively. On the basis of these results, the measurement of small-angle dynamic light scattering was performed in the range of frequency from 100 Hz–10 kHz. To avoid excessive heating, the applied driving voltage was fixed at E = 1.71 V/cm in all measurements of small-angle light scattering. All of the measurements were performed 10 min after application of the electric field to ensure that the system was in a steady state.

Results and discussion

A series of micrographs in Fig. 3 shows the electric field-induced phase separation and the evolution of the domain morphology in an ionic SDS micellar solution under a sinusoidal electric field. Driving voltage of $E \simeq 3.3$ V/cm at the frequency of f = 1 kHz was applied in this observations. These photographs were taken in a one-phase region at the temperature distance $T_p - T \simeq 500$ mK, and the scale in the pictures is 500 μm. The photograph at Fig. 3A shows a homogeneous state before the sinusoidal electric field was applied. The photograph at Fig. 3B shows the liquid-liquid phase separation induced by application of the electric field. After the phase separation, the concentration domains form very complex structures as seen in the

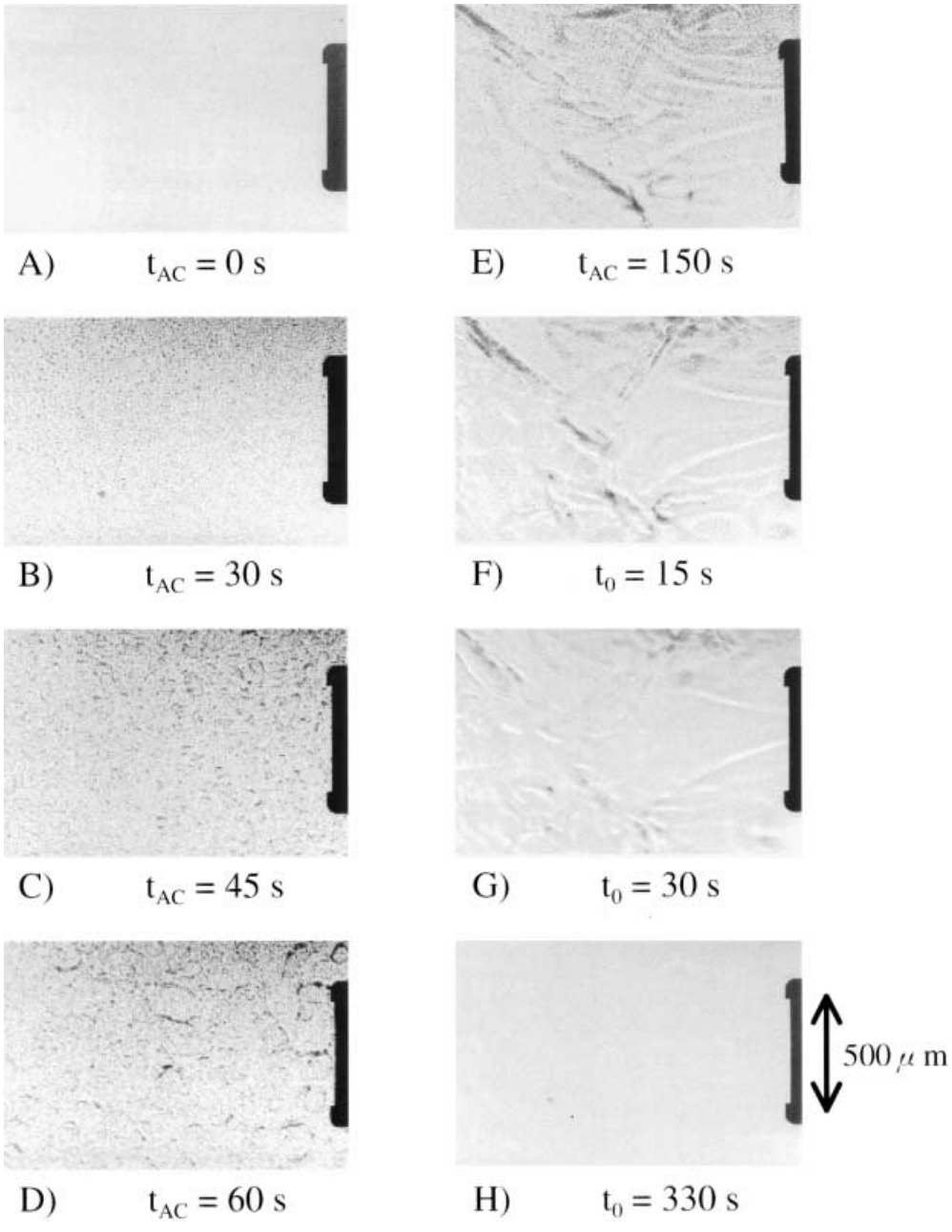

Fig. 3A–H Evolution of the concentration domains morphology under a sinusoidal electric field. The electric field was applied at time $t = 0$ and stopped at time $t = 150$. Photographs of the sinusoidal electric field-induced phase separation: **A** in a quiescent state; **B** $t_{AC} = 30$ s; **C** $t_{AC} = 45$ s; **D** $t_{AC} = 60$ s; **E** $t_{AC} = 150$ s after application of the electric field; **F** $t_0 = 15$ s; **G** $t_0 = 30$ s; **H** $t_0 = 180$ s after cessation of the electric field application

photographs at Figs. 3C–E taken at $t_{AC} = 45$ s, $t_{AC} = 60$ s, and $t_{AC} = 150$ s after the field application, respectively.

Electric field-induced phase separation was considered to be characteristic of the system under a sinusoidal electric field and was attributed to the electric field-induced instability. A charged interface between the ionic micelle-rich and -poor phases is formed by the phase separation. Electrostatic repulsion between charges would decrease interfacial tension. The shape of the interface will be deformed by the electric field due to charges at the interface coupled with the application of an external AC field through the electrodes. The structure formation shown in the photographs at Fig. 3C, D was observed throughout the frequency range $f = 100$ Hz $\sim$ 10 kHz [18]. The concentration domain morphology under a sinusoidal electric field observed here was different from those observed for polymer blends under a DC electric field observed by Venugopal and Krause [19]. The characteristic concentration domains disappeared after cessation of the applied electric field as shown in the photographs at Fig. 3F–H, which were taken at $t_0 = 15$ s, $t_0 = 30$ s, and $t_0 = 180$ s after cessation of the applied field, respectively.

Thus, the photographs at Fig. 3 provide clear evidence that the electric field induces phase separation in a solution that is originally a homogeneous one-phase in a quiescent state. We preliminary investigated the phase separation temperature shift $T_p - T_{p,E}$ by observing the spinodal ring with the Zetaplus Brookhaven electrodes cell. Here, $T_{p,E}$ corresponds to phase separation temperature under a sinusoidal electric field. The temperature shifts $T_p - T_{p,E}$ are approximately 0.05 K at the driving voltage E = 1.71 V/cm at each frequency. Thus, the temperature shift is a reflection of an unusual fluctuation occurring under a sinusoidal electric field. These results imply that there is dynamical coupling between the concentration fluctuation and applied sinusoidal electric field. Phase separation temperature shifts in the presence of a DC electric field have been demonstrated in experimental studies by Wirtz and Fuller [8] and Debye and Kleboth [14] and also in a theoretical study by Onuki [6]. According to Debye and Kleboth, the amount of free energy change is proportional to the square of the applied driving voltage, and, consequently, the phase separation temperature shifts by $|T_c - T_{c,E}| \simeq 0.015$ K at the electric field intensity of 45,000 V/cm in a nitrobenzen-2,2,4-trimethylpentane system [14]. On the other hand, Wirtz and Fuller [8] reported electric-induced mixing in critical solutions of polystyrene in cyclohexane and in poly(*p*-chlorostyrene) in ethylcarbitol, the binary mixtures of which form UCST and LCST solutions, respectively. They also found that the phase-separation temperature shift is proportional to the square of the applied driving voltage. In a DC electric field, however, the phase-separation temperature shift is small even if the applied field is large. Therefore, our experimental results indicate that the application of an AC field is much more effective for an electric field-induced phase separation than is the application of a DC field. To the best of our knowledge, this is the first report of a temperature shift under a sinusoidal electric field, attributed to coupling phenomena between concentration fluctuation and the sinusoidal electric field.

Figure 4 shows a typical autocorrelation function $g^{(2)}(\tau) - 1$ for an SDS micellar solution under a sinusoidal electric at the temperature distance from phase separation point $T_P - T \simeq 0.1$ K [20]. Here, the applied field frequencies are $f = 100$ Hz, 1 kHz, 10 kHz, and E = 0 V/cm. At zero-electric field, the autocorrelation function had an exponential-like decay. The autocorrelation function in a sinusoidal electric field seems to be described by an exponentially damped cosine oscillation. Maximum values of the first peak of the oscillatory part in $g^{(2)}(\tau) - 1$ coincide with those without the sinusoidal electric field, except for $g^{(2)}(\tau) - 1$ at f = 10 kHz. When the applied frequency f was changed, the amplitude and period of the oscillatory part of $g^{(2)}(\tau) - 1$ were also changed. The amplitude of the oscillatory part was smallest at $f = 1$ kHz. This suggests the existence of a component that can possible to couple to an applied frequency. Figure 5 shows the temperature dependence of the correlation function at the applied frequency of 100 Hz. At $T_P - T \simeq 0.97$ K, the oscillatory part existed only in the long time foot of the correlation function, which is in contrast with that observed at $T_P - T \simeq 0.10$ K. Damped oscillation has been observed by electrophoretic dynamic light scattering or quasielastic dynamic light scattering in the presence of a

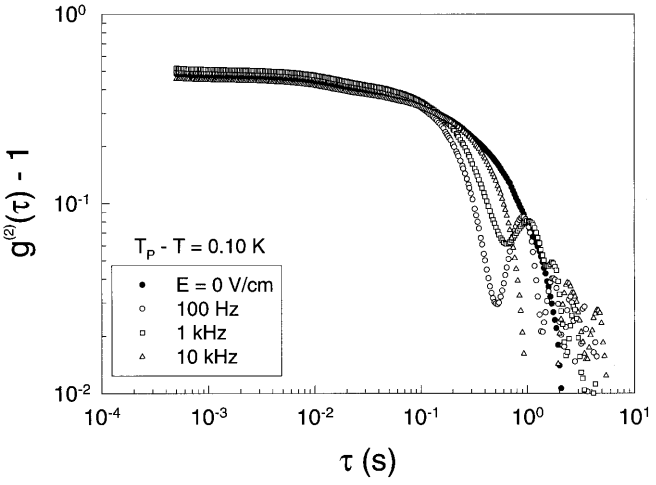

Fig. 4 The correlation function in the presence of a sinusoidal electric field at the frequency of f = 100 Hz (*circles*), 1 kHz (*squares*), and 10 kHz (*triangles*) with driving voltage E = 1.71 V/cm, and without an electric field E = 0 V/cm (*filled circles*), at the temperature distance of T_p - T = 0.10 K and scattered angle $\theta = 3.1°$

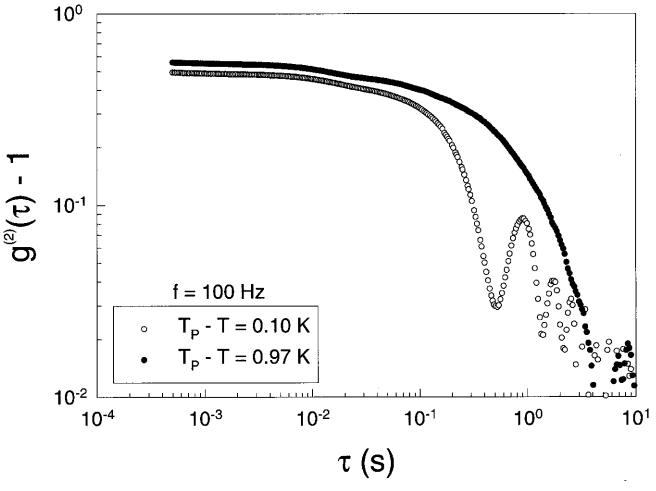

Fig. 5 Temperature dependence of the correlation function in the presence of a sinusoidal electric field at the frequency of f = 100 Hz with driving voltage E = 1.71 V/cm. The temperature distances from phase separation temperature T_p – T are 0.10 K (*circles*) and 0.97 K (*filled circles*), respectively

sinusoidal electric field, referred to as QELS-SEF [21–26]. In the QELS-SEF method, formulation for data analysis has been attempted by several authors, though the substantial concepts are almost the same [21–25]. Robertson derived the correlation function in a homodyne mode by introducing the coupling of oscillating electrophoresis of particles in sinusoidal electric field and diffusion by random force [23]. We have tried to fit our data to the formula of QELS-SEF derived by Robertson. However, it was impossible to fit our data to Robertson's formulation. If the oscillatory part is due to the electrophoresis of micellar molecules itself, as was assumed by Robertson, oscillation should also appear in a shorter time region in the correlation function, due to the Doppler shift, which is attributed to a movement of the particle itself. Oyama et al. studied a suspended solution system of an imogolite, which is a rod-like molecule, under a sinusoidal strain. They presented decay curves with exponentially damped cosine oscillations, and they attributed the oscillation to the rotational motion of the rod-like molecule [27]. It is concluded that the damped oscillation in the correlation function observed here could not be categorized into one of those presented in the literature. Figure 6 shows the temperature and applied frequency dependencies of both the characteristic time, τ_o, and the reciprocal of an apparent period of the oscillatory part, f_o. τ_o was determined as the time at which the first minimum appears. f_o was determined from the difference in the time at a peak and that at the next peak. In Fig. 6a, the period f_o was almost independent of applied frequency at $T_P - T \simeq 0.97$ K. When the temperature approaches the phase separation point, the applied frequency dependence of f_o became remarkable. Near the phase separation point, the applied frequency dependence of f_o remained almost constant, but it did not depend on temperature in the range of $0.10 < T_p - T < 0.24$ K. The characteristic correlation time τ_o was shifted to the shorter time side with the approach to the phase separation point, as shown in Fig. 5. The correlation length of concentration fluctuation generally increases with temperature approaching the phase separation point. It seems reasonable to assume that the temperature dependence of τ_o was related to the change in the correlation length of the concentration fluctuation. These results therefore suggest the existence of a dynamic coupling phenomenon shown in Fig. 3. Since the photographs in Fig. 3 show the development of concentration fluctuation due to sudden application of an AC electric field, the time scale in the morphology development does not correspond to the time scale of damping oscillation in the correlation function, which represented the concentration fluctuation itself and was measured in a steady state.

Electric field-induced phase separation is thought to be related to the dynamic coupling effects, as seen in the morphology observations. The deformation of the concentration domain shown in Fig. 3 suggests an electric field-induced enhancement and deformation of the concentration fluctuation, i.e., an ionic SDS micelles-rich phase. The damping oscillation in the correlation function in the long time region is thought to be due to migration and deformation of the concentration fluctuations by the electric field, across the irradiated volume by the incident laser beam. Since the size of the critical fluctuation increases with decreases in the temperature difference, $T_p - T$, the fluctuation size at $T_p - T = 0.97$ K is the smallest among those measured at different values of $T_p - T$, and the decay rate at $T_p - T = 0.97$ K is also the fastest. Then, the critical fluctuation at $T_p - T = 0.97$ K would not be affected by the applied frequency. On the other hand, near the phase-separation temperature, $T_p - T = 0.10$ K, the critical fluctuation has a long-range slow structure. The slow structure of the critical fluctuation would dynamically migrate with the applied frequency. As a result of the migration of the critical fluctuation, the critical fluctuation may be enhanced.

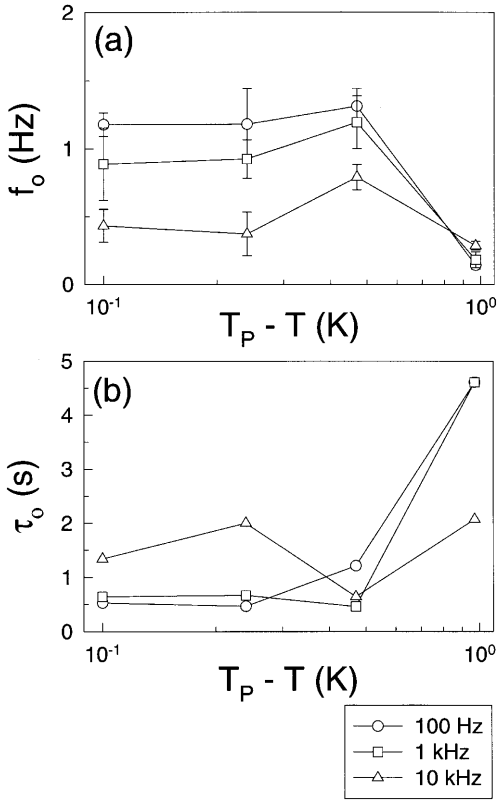

Fig. 6 a The average period of the oscillatory parts f_o in the correlation function as a function of temperature at the indicated frequency of an applied sinusoidal electric field. **b** The characteristic time τ_o at which the oscillatory part appears as a function of the applied frequency and temperature. τ_o was determined as the time of the first minimum in each correlation function. *Circles*, *squares*, *and triangles* correspond to the values at the frequencies of 100 Hz, 1 kHz, and 10 kHz, respectively. The *solid line* is a guide for the eye

The enhanced fluctuation contributes as a driving force to phase separation. Detailed investigation of the spinodal decomposition process under an AC electric field is needed.

As mentioned above, the sinusoidal electric field-induced phenomena seem to be affected significantly near the phase separation point, just as the shear-induced critical phenomenon [2–5]. Hence, both f_o and τ_o as a function of the applied frequency would be attributed to the deformation of the concentration fluctuation, which increases as a function of temperature rather than electrophoresis of micelles itself. Although the detailed mechanisms of correlation function with a damped cosine mode cannot be explained, the results in this study suggest the existence of a dynamic coupling phenomenon between sinusoidal electric field and concentration fluctuation. Then, the universal scaling law may be applicable to an electric field-induced critical phenomenon.

Acknowledgements This project was performed under the control of Prof. K. Hamano. We are very sorry that he passed away at the final stage of this work. We are grateful to Prof. H. Ushiki of Tokyo Agriculture and Technology University for his fruitful discussions and enlightening comments on the subject.

References

1. Hamano K, Ducros E, Louisor E, Rouch J, Tartaglia P (1996) Physica A 231:144
2. Onuki A, Kawasaki K (1979) Ann Phys (NY) 121:456
3. Onuki A (1997) J Phys Condens Matter 9:6119
4. Hamano K, Ushiki H, Tsunomori F, Sengers JV (1997) Int J Thermophys 18:379
5. Hamano K, Isii T, Ozawa M, Sengers JV, Krall AH (1995) Phys Rev E 51:1254
6. Onuki A (1995) Europhys Lett 29:611
7. Wirtz D, Berend K, Fuller GG (1992) Macromolecules 25:7234
8. Wirtz D, Fuller GG (1993) Phys Rev Lett 71:2236
9. Isojima T, Kato H, Hamano K (1998) Phys Lett A 240:271
10. Goldburg WI, Min KY (1994) Physica A 204:246
11. Fujii S, Isojima T, Hamano K (1999) Phys Lett A 263:393
12. Moses E, Kume T, Hashimoto T (1994) Phys Rev Lett 72:2037
13. Kameyama K, Takagi T (1990) J Colloid Int Sci 140:517
14. Debye P, Kleboth K (1965) J Chem Phys 42:3155
15. Rzoska SJ, Rzoska AD, Ziolo J (2000) Phys Rev E 61:960
16. Isojima T, Fujii S, Kubota K, Hamano K (1999) J Chem Phys 111:9839
17. Uzgiris EE (1974) Rev Sci Instrum 45:74
18. Fujii S, Isojima T, Hamano K (1998) Rep Prog Polym Phys Jpn 41:83
19. Venugopal G, Krause S (1992) Macromolecules 25:4626
20. Fujii S, Isojima T, Hamano K (1999) Rep Prog Polym Phys Jpn 42:113
21. Ware BR, Flygare WH (1971) Chem Phys Lett 25:81
22. Ware BR, Flygare WH (1972) J Colloid Int Sci 39:670
23. Robertson B (1991) J Chem Phys 95:3873
24. Imaeda T, Kimura Y, Kohzo I, Hayakawa R (1994) J Chem Phys 100:950
25. Schmitz KS, Pontalion TJ (1995) J Chem Phys 103:794
26. Bern BJ, Pecora R (1976) Dynamic light scattering. Wiley, New York
27. Oyama Y, Takada A, Nemoto N (1999) Nihon Reoroji Gakkaishi 27:249